HHS Public Access

Author manuscript

Ocul Surf. Author manuscript; available in PMC 2024 November 22.

Published in final edited form as:

Ocul Surf. 2021 October ; 22: 86–93. doi:10.1016/j.jtos.2021.07.009.

Anterior segment optical coherence tomography angiography in the assessment of ocular surface lesions

William W. Binotti[a,b], **Huan Mills**[c], **Ricardo M. Nosé**[a,b], **Helen K. Wu**[b], **Jay S. Duker**[c], **Pedram Hamrah**[a,b,*]

[a]Center for Translational Ocular Immunology, USA

[b]Cornea Service, Department of Ophthalmology, Tufts Medical Center, Tufts University School of Medicine Boston, MA, USA

[c]Department of Ophthalmology, New England Eye Center, Tufts Medical Center, Tufts University School of Medicine, Boston, MA, USA

Abstract

Purpose: Describe the utility of anterior segment optical coherence tomography angiography (AS-OCTA) to assess ocular surface lesions.

Methods: Retrospective, case-control study of 10 eyes of 9 patients with malignant lesions and 23 eyes of 22 patients with benign lesions. Lesions included 13 epithelial, 10 pigmented and 10 lymphoid lesions. Graders performed an average of 3 depth and diameter measurements of peri-lesional vessels entering each lesion on AS-OCTA. Statistical models to assess differences between groups accounted for bilateral eye inclusion and lesion thickness (on AS-OCT). Receiver operating characteristic (ROC) curve and area under the curve (AUC) were performed for each parameter.

Results: In the benign and malignant groups, age was 49.5 ± 22.4 and 64.3 ± 10.6 years ($p = 0.145$) with 45% males and 55% males ($p = 0.458$), in their respective groups. AS-OCTA showed greater peri-lesional vessel depth and diameter in malignant lesions (315.2 ± 73.0 μm, $p < 0.001$ and 76.4 ± 18.2 μm, $p < 0.001$; respectively) compared to benign lesions (199.4 ± 34.1 μm and 44.0 ± 9.4 μm, respectively). Malignant lesions showed deep and dilated peri-lesional vessels, which may represent feeder vessels. Vessel depth showed AUC = 0.980, 90.9% sensitivity and 100.0% specificity with a 236.5 μm cutoff. Vessel diameter showed AUC = 0.960, 100.0% sensitivity and 88.9% specificity with a 53.9 μm cutoff.

Conclusion: AS-OCTA shows greater peri-lesional vessel depth and diameter of malignant lesions compared to benign lesions. This imaging modality provides novel and non-invasive functional vascular parameters that can potentially aid the assessment of ocular surface lesions.

*Corresponding author. New England Eye Center, Tufts Medical Center, 800 Washington St. Box #450, Boston, MA, 02111, USA. phamrah@tuftsmedicalcenter.org, pedram.hamrah@tufts.edu (P. Hamrah).

Declaration of competing interest

WWB, HM, RMN, HKW: no disclosures; JSD: Carl Zeiss Meditec, Inc. (Dublin, CA, USA) (S), Optovue, Inc. (Fremont, CA, USA) (S), PH: Heidelberg Engineering (Heidelberg, Germany) (C, S).

Appendix A. Supplementary data

Supplementary data to this article can be found online at https://doi.org/10.1016/j.jtos.2021.07.009.

Keywords

Conjunctival tumors; Optical coherence tomography angiography; AS-OCTA; Feeder vessel; OCTA; Ocular surface neoplasia

1. Introduction

Benign or malignant conjunctival tumors, or ocular surface lesions, are generally classified as melanocytic and non-melanocytic [1]. The latter can be further sub-categorized into epithelial, lymphoid, vascular, lipomatous, fibrous, myogenic, histiocytic, neural, metastatic and secondary tumors [1–3]. These lesions are generally diagnosed through their clinical features, history, risk factors, evolution, location, and confirmed through histopathology [1,4,5]. Morphological lesion characteristics on slit-lamp examination, such as anatomical location, basal diameter, pigmentation, presence of cysts or feeder vessels, have been used to distinguish benign from malignant tumors [6].

The benefits of complimentary diagnostic imaging have been demonstrated for the assessment of these lesions. Ultrasound bio-microscopy, for example, is commonly used to determine the intraocular tumor invasion depth and metastasis, showing limited image resolution with good tissue penetration for the anterior segment [7–9]. Its main disadvantages are the axial resolution, limited accessibility to this imaging technique, the need for submersion and contact under topical anesthesia, and experienced operator for image acquisition [10,11]. The study of the vasculature pattern in ocular tumors may provide additional insight into diagnosis and prognosis of tumors [12]. Although this concept is well established in chorioretinal tumors, studies on anterior segment tumors are scarce [13]. Brunner et al. have recently described the vascular characteristics of ocular surface neoplasia as assessed by indocyanine green angiography (ICGA) [14]. They analyzed epithelial and pigmented lesions, and provided measurements, such as mean vessel diameter, lesion filling times, and quantification of afferent and efferent vessels, with a significantly decreased lesion filling time in malignant lesions, compared to benign lesions.

Anterior segment-optical coherence tomography (AS-OCT) is a non-invasive and non-contact device that can generate high-resolution cross-sectional B-scans of the ocular surface, using near-infrared light with an approximately 5 μm axial resolution [15]. In ocular surface squamous neoplasia (OSSN), it has previously been used to assess the lesion thickness and epithelial thickness [11,16]. The limitation of AS-OCT, however, is the inability to provide functional parameters, such as blood flow. Furthermore, the novel AS-OCT angiography (AS-OCTA) is capable of detecting blood vessel flow (by calculating decorrelation signals) from the red blood cell movement within the vessels through sequential *en face* scans at the same location. This modality is now widely used in retinal vascular diseases [17] and recently for intraocular tumors [18,19]. The main disadvantages of OCTA, unlike other angiography techniques with dye injection, are the inability to accurately determine venous from arterial and to detect vessel leakage.

The application of AS-OCTA has shown promising results in corneal neovascularization and other ocular surface diseases [20,21]. However, the utility of AS-OCTA in ocular

surface tumors remains underexplored. We hypothesize that this novel feature can provide qualitative and quantitative vascular parameters that can aid in the assessment of ocular surface lesions. The aim of this study is to investigate vascular depth and diameter as assessed by AS-OCTA in ocular surface lesions, and to explore if these parameters demonstrate significant differences between malignant and benign lesions. Herein, we describe the preliminary utility of this technology in the setting of ocular surface tumors.

2. Methods

2.1. Patient selection

The OCT database and clinical records of patients with conjunctival lesions in which AS-OCTA imaging was performed for clinical purposes at the Cornea Service, New England Eye Center, Department of Ophthalmology, Tufts Medical Center, Boston, Massachusetts, were reviewed between November 2016 and December 2019. Inclusion criteria were patients with diagnosis of ocular surface lesions on clinical records with AS-OCTA scans of the lesion. In order to explore the utility of AS-OCTA imaging in ocular surface tumors, a wide range of lesions were included: epithelial tumors, such as invasive OSSN, non-invasive OSSN, i.e. conjunctival intra-epithelial neoplasia (CIN), pterygium and pingueculum; pigmented lesions, such as melanoma, primary acquired melanosis (PAM) with or without atypia, nevus, and congenital or complex-associated melanosis; and lymphoid lesions, such as lymphoma, benign reactive lymphoid hyperplasia (BRLH), conjunctival granuloma and inclusion cyst. In the benign group, pterygium/pingueculum, conjunctival granuloma and inclusion cyst were included for comparison purposes, since these can clinically often resemble malignant lesions [6]. The above malignant tumors were included, as they represent the 3 most common tumor categories [6]. The exclusion criteria were lesions with indication for excisional biopsy due to malignancy suspicion that lost follow-up or lack of a documented histopathology report and images with excessive artifacts that did not allow vessel analysis in the region of interest.

A total of 39 eyes of 36 patients were reviewed, of which 33 eyes of 31 patients were included. This retrospective, cross-sectional study was approved by the Tufts Medical Center/Tufts University School of Medicine institutional review board (IRB #13216), adhered to the tenets of the Declaration of Helsinki, and was compliant with Health Insurance Portability and Accountability Act (HIPAA). Three eyes of 3 patients with indication for biopsy were excluded due to loss of follow-up and 3 eyes of 2 patients were excluded due to excessive motion artifacts on AS-OCTA. Patients with benign lesions included pterygium, pingueculum, nevus, racial melanosis, conjunctival granulomas, inclusion cysts and BRLH. Of these, 7 patients underwent excisional biopsies. The main clinical indications for biopsy in this group were rapid growth, local invasion, imprecise boarders, increased vascularization, patient history, and esthetic appearance. Malignant lesions included non-invasive OSSN (i.e. CIN), OSSN, melanoma, and lymphoma and all malignant cases were biopsy-proven.

2.2. Imaging technique

Subjects had undergone anterior segment imaging on the Avanti XR AngioVue (Optovue, Inc., Fremont, CA) with the projection-resolved algorithm as previously described [22]. In short, since the high-intensity flow signal from the superficial layers can project artifacts into the deeper layers, the software suppresses the smaller intensity peaks from superficial flow that dissipate into the subsequent deeper layers in the same transverse location, thereby decreasing their projection artifacts to the deeper layers. The system acquired volumetric scans of 400 × 400 B-scans at 70,000 A-scans per second, using a light source centered on 840 nm and a bandwidth of 45 nm with a 5 μm axial resolution and a 15 μm transverse resolution. The AngioVue 6 × 6mm HD Retina scan was performed with the long corneal adaptor module lens attached and manual adjustments of the Z motor, P motor and focus to obtain a clear image of the anterior segment. The volumetric scans generate an *en face* image, with a coronal view of the ocular surface structures, and an angiogram image with the blood flow of the anterior segment vessels. The scans centered on the conjunctival lesion's location (i.e. nasal, temporal, caruncle, fornix) were selected for analysis.

2.3. Imaging analysis

On AS-OCTA, the vessels entering the lesion were analyzed with their lesion boundaries established by *en face* images, as shown in Figs. 1 and 2. To assess the repeatability of this method, 3 vessels that entered the lesion were randomly selected by 2 blinded graders in order to provide an average value per grader for each parameter. The selected vessels were measured for depth and diameter at the point of entry in the lesion, therefore they were peri-lesional vessel parameters. The average vessel depth (μm) of the 3 most representative vessels was performed on the OCT device, with the segmentation (zero reference) based on the non-affected surface of the eye, ergo peri-lesional area. For vessel diameter measurements, the AS-OCTA images were exported with their pixel-ratio preserved and then converted into micrometers using FIJI software [23]. Next, one vessel diameter measurement per selected vessel was performed, at the point of entry and perpendicular to the vessel direction, where the average of the 3 measurements was used to represent the peri-lesional vessel diameter (Figs. 1 and 2). Further, the OCT cross-sectional scan at the apex of the lesion was selected and the maximum lesion thickness was measured from the epithelial surface to the posterior border of the lesion, in order to assess a potential confounding factor. All quantitative measurements were performed on de-identified images by 2 graders (WB and HM), masked to the diagnosis and to grader's measurements. In case of greater than 15% discordance between measurements, a third grader (RN) performed measurements and the average of the 3 graders was used for analysis. All measurements were repeated on the same set of images, at a different time, under the same conditions by the same grader (WB) to determine the intra-grader agreement. The description and nomenclature of the vessels were based on their anatomical location and observational AS-OCT studies [24–27].

2.4. Statistical analysis

Statistical analyses were performed using Statistical Package for the Social Sciences software (ver. 17, SPSS Inc., Chicago, IL, USA), the data was represented as mean ±

SD and p-values <0.05 were considered statistically significant. A Mann-Whitney U tests were performed on age and lesion thickness to assess differences between benign and malignant group. Chi square test was performed on the gender distribution between groups. Generalized estimated equations were performed to assess differences in vessel depth and vessel diameter between groups, accounting for bilateral eye inclusion and individual lesion thickness to avoid confounding factors. Therefore, vessel depth or diameter were entered as separate dependent variables, groups as independent factors with Bonferroni corrections and thickness as a covariate.

Furthermore, to demonstrate the sensitivity and specificity of the vascular parameters, receiver operating characteristic (ROC) curves with their area under the curve (AUC) were performed to further assess their application and optimal cutoff points. In addition, intra-grader and inter-grader repeatability of the quantitative parameters, intraclass correlation coefficients (ICC) were performed on the measures within same grader and between graders, respectively, with their 95% confidence interval [lower bound – upper bound].

3. Results

3.1. Demographics

In the benign group a total of 23 eyes (22 patients) were included and in the malignant a total of 10 eyes (9 patients). All lesions in the malignant group were biopsy proven. There was no significant difference between the groups regarding the mean age (49.5 ± 22.4 and 64.3 ± 10.6 years, respectively; $p = 0.145$) and the gender distribution with 45.0% and 55.0% males in the respective groups ($p = 0.458$). The demographic data f the benign and malignant groups is displayed in Table 1 and lesion thickness in Supplemental Table S1.

3.2. Quantitative AS-OCTA parameters

The representative AS-OCTA images of benign and malignant lesions are shown in Figs. 1 and 2, respectively, and their quantitative parameters in Fig. 3. Overall, the malignant lesions on AS-OCTA showed increased peri-lesional vessel depth (315.2 ± 73.0 μm, $p < 0.001$) compared to benign lesions (199.4 ± 34.1 μm), demonstrating that malignant lesions show deeper vessels entering the tumor, even when accounting for the individual lesion thickness. Malignant lesions also showed greater peri-lesional vessel diameter (76.4 ± 18.2 μm, $p < 0.001$), e.g. more dilated, compared to benign (44.0 ± 9.4 μm), when accounting for lesion thickness. For both statistical analysis, age and gender were not significant factors ($p \geq 0.05$) and therefore not included in the models.

In this study, peri-lesional vessel depth showed an AUC of 0.980 (ROC curve shown in Supplemental Fig. S1). When establishing a sensitivity >90%, peri-lesional vessel depth showed a sensitivity of 90.9% and specificity of 100.0% with a cutoff at 236.5 μm (1 CIN case with low grade dysplasia showed a 225.0 μm depth). In contrast, peri-lesional vessel diameter showed an AUC of 0.960 (ROC curve shown in Supplemental Fig. S1). When establishing a sensitivity >90%, peri-lesional vessel diameter showed a sensitivity of 100.0% and specificity of 88.9% with a cutoff at 53.9 μm (1 inflamed pterygium showed 60.5 μm and 1 inflamed conjunctival inclusion cystic showed 68.3 μm diameter). In general, deeper

vessels entering the lesion were noted in malignant lesions, which branched from the deep conjunctival stroma and the episcleral regions. In contrast, these deep vessels were not evident in benign lesions and their perilesional vessels entered more superficially within the conjunctiva (i.e. substantia propria). The selected vessels in malignant lesions also showed increased diameter compared to benign lesions and may represent feeder vessels.

3.3. Parameters within lesion subcategories

The measurements for each lesion subtype (i.e. epithelial, pigmented and lymphoid) are shown in Table 2. The mean peri-lesional vessel depth and diameter were significantly greater in malignant epithelial and pigmented tumors. The malignant epithelial group showed a 1.4-fold ($p = 0.005$) and a 1.6-fold increase ($p = 0.003$) in the peri-lesional vessel depth and diameter, respectively, whereas the malignant pigmented lesions a 1.7-fold ($p = 0.036$) and a 1.8-fold increase ($p = 0.036$), respectively. Although the number of eyes in the malignant lymphoid group ($n = 2$) was insufficient for statistical analysis, there was a 1.9-fold and a 2.2-fold increase in vessel depth and diameter, respectively.

Of note, for all malignant epithelial lesions, the peri-lesional vessel depth was >231.0 μm, except for 1 non-invasive OSSN (CIN) case (225.0 μm), and vessel diameter was >55.7 μm, including the abovementioned CIN case. Also, all malignant pigmented lesions showed peri-lesional vessel depth and diameter >220.0 μm and >65.1 μm, respectively. Further, all lymphoid malignant lesions showed vessel depth and diameter >430.0 μm and >68.3 μm, respectively. While feeder vessels were not noted clinically in 2 non-invasive OSSN (CIN) cases, AS-OCTA still demonstrated superficial vessels beneath the lesion arising from limbal arcade vessels (233.5 ± 12.0 μm) with increased vessel diameter (59.4 ± 5.3 μm) compared to the pterygium/pingueculae cases (192.5 ± 25.4 μm and 44.8 ± 7.3 μm, respectively) without clear connections to the underlying episcleral vessels, highlighted in Supplemental Fig. S2. In contrast, the invasive OSSN case showed deep and dilated vessels entering the lesion (368.0 μm and 74.8 μm, respectively), shown in Supplemental Fig. S3. In the PAM with atypia case, small tortuous vessels were noted surrounding small and diffusely pigmented lesions on clinical records, which were deep (257.0 μm) and dilated (64.7 μm) stroma conjunctival vessels on AS-OCTA, seen in Suuplemental Fig. S4, in contrast to the superficial (177.0 ± 49.6 μm) and thinner (38.9 ± 6.2 μm) conjunctival vessels noted in benign pigmented lesions (Fig. 1). Therefore, malignant lesion subcategories also showed a consistent increase in peri-lesional vessel depth and diameter.

3.4. Morphological vessel assessment

The vessels entering malignant lesions were noticeably tortuous and dilated in all malignant cases, except in 2 non-invasive OSSN (CIN) cases, and were morphologically similar to previous descriptions of feeder vessels [28]. Graders had a tendency to perform vessel depth and diameter measurements on these distinguishing vessels entering the lesion. All CIN cases showed rich vascularization beneath and surrounding the lesion with vessels entering the lesion, branching from the episcleral and/or deep stroma conjunctiva (Fig. 2). Furthermore, only scant and small intra-lesional vessels were noted mostly at the borders of the conjunctival lesion, where the deep feeder vessels were identified and measured. The 2 CIN cases without clinically noted feeder vessels showed no intra-lesional vessels, but

rich peri-lesional vascularization. Distinguishing features of the latter from benign epithelial lesions were that vessels surrounding the lesion base at the limbus appeared slightly dilated and tortuous with distinct branching from the deep limbal arcade vessels towards the lesion as opposed to straight, thin and superficial conjunctival vessels towards the “head” of the pterygium/pinguecula cases, shown in Supplemental Fig. S2. In the invasive OSSN case, there was extensive tumor infiltration over the bulbar conjunctiva and cornea with many deep, dilated, and tortuous vessels from the episclera and deep conjunctival stroma entering the lesion. The vessels within the epithelial tumor (intra-lesional) at the bulbar and limbal conjunctiva were irregular and scarce with many terminal vessels (noted as pinpoint blood flow on AS-OCTA), whereas the intra-lesional corneal vessel showed a “sea-fan” pattern, shown in Supplemental Fig. S3.

In malignant pigmented lesions, dilated and deep stroma conjunctival vessels were noted entering the melanoma lesions (Fig. 2) or at the base of PAM with atypia lesion (Supplemental Fig. S4), but not in benign pigmented lesions. Moreover, in the lymphoid subtype, BRLH cases mostly showed conjunctival vessels surrounding the lesion with few fine stroma conjunctival vessels at the lesion base (Fig. 1). However, in the lymphoma case, there was episcleral vessel involvement with deep and dilated vessels entering the base of the lesion, despite the thin overlying vessels at the anterior surface of the lesion (Fig. 2).

In summary, vessel depth and diameter measurements in malignant lesions showed presence of deep, dilated and tortuous peri-lesional vessels, which could represent feeder vessels.

3.5. Repeatability of AS-OCTA parameters

There was a high intra-grader repeatability for the vessel depth and diameter measurements (ICC = 0.994 [0.936–0.999] and ICC = 0.977 [0.938–0.992], respectively). There was also a high inter-grader repeatability the measures with ICC = 0.982 [0.955–0.993] and ICC = 0.977 [0.919–0.992], respectively. Interestingly, graders did not always measure the same exact vessels due to their random selection. Nonetheless, the average measurements of the vessels showed high ICC values in all analysis. This observation might reflect the focal vascular changes that occur in malignant lesions, whereas vessels entering the benign lesions were from the superficial conjunctival plexus.

4. Discussion

Herein, we report that the peri-lesional vessel depth and diameter of ocular surface lesions can be assessed objectively with AS-OCTA, with high repeatability. A significant increase of peri-lesional vessel depth and diameter was shown in malignant lesions and could be potential parameters to help distinguish them from benign lesions of the ocular surface. Our results herein highlight a high sensitivity and specificity (with high AUC) of this novel technology, adapted for the anterior segment, to help differentiate such lesions.

Identifying feeder vessels is an important clinical sign and can often be a defining feature for malignant conjunctival tumors [4,6]. These are often described as dilated and tortuous vessels with abnormal bulges, arteriolar-venous shunts or loops [28]. Brunner et al. reported decreased intralesional blood filling time on ICGA in malignant lesions, but not vessel

diameter or number of afferent and efferent vessels, as compared to benign lesions [14]. We show that malignant tumors have a greater peri-lesional vessel depth and diameter, and that these vessels could represent feeder vessels as noted clinically on slit-lamp. As highlighted by Brunner et al. there can be a discrepancy between feeder vessels identified on slit-lamp compared to fluorescent angiography, where the former were most commonly identified efferent vessels from the lesion rather than the “feeder” afferent vessel on angiography [14]. A disadvantage of OCTA is its current inability to determine the direction and velocity of blood flow. However, the clinical importance of correctly identifying these anomalous vessels as afferent or efferent in malignant conjunctival lesions is yet to be determined. Nevertheless, our study highlights novel AS-OCTA vascular features that can potentially help distinguish between benign and malignant conjunctival lesions without the time-consuming and invasive dye angiography, which poses side effects ranging from mild to potentially life-threatening [29,30]. However, studies establishing the relation of AS-OCTA and fluorescent angiography findings between benign and malignant ocular surface lesions are warranted.

Considering that the vessels measured were not intra-lesional, but rather vessels of the adjacent conjunctiva prior to entering lesions (e.g. peri-lesional), it is not surprising that the lesion thickness did not significantly affect with the vessel depth analysis (Supplemental Table 1). Thus, the depth is mainly a representation of the vascular plexus location that originated the feeder vessel (based on the anatomical and observational AS-OCT studies of the ocular surface) [26,27]. In contrast, when analyzing the intra-lesional vasculature, one should consider the lesion thickness to determine the relative lesion depth of the vessels. A recent AS-OCTA case series on OSSN lesions by Liu et al. reported a higher vascular density beneath the conjunctival lesion (sub-epithelial) compared to the intra-lesional vessels [31]. In our study, the OSSN case shows a similar “sea fan” pattern of intra-lesional vessels over the cornea and an irregularly vascularized network at the limbus and bulbar conjunctiva. We noted that both the intra-lesional corneal and conjunctival vessels show direct connections to deep episcleral vessels. The high vascularity and connections to the sub-lesional vascular plexi suggests the local effects of angiogenesis necessary for tumor growth and present in malignant neoplasia [32,33].

In our study, automated vessel density calculations were not performed due to segmentation errors of the device’s OCTA software (designed for posterior segment of the eye) and shadowing artifacts that can affect the vessel density measurement, especially in pigmented lesions. Further, a global vessel density measurement of the conjunctival vessels may underestimate the focal vascular changes that occur in malignant lesions. Therefore, we chose to measure only peri-lesional vessels at the point of entry of the lesion to provide an easy and identifiable landmark in order to facilitate clinical translation. Our results herein indicate that feeder vessels entering malignant lesions may originate from the episclera and deep stroma of the conjunctiva, whereas in benign lesions the peri-lesional vessels originate within the superficial stroma of the conjunctiva with no clear deep branching from the intra-lesional vessels.

Interestingly, in the non-invasive OSSN (CIN) cases without clinically evident feeder vessels, although the peri-lesional vessels are within the superficial conjunctiva, they

appeared slightly dilated, irregular, and branching from episcleral vessels at the limbus. This contrasts with the thin and straight superficial conjunctival vessels overlying the limbus in pterygium/pingueculae. In addition, invasive OSSN shows deep and dilated episcleral vessels with high intra-lesional vascularity. In the PAM with atypia case, the vessels are mainly within the conjunctival substantia propria; however, the vessels at the lesion base appear dilated and tortuous (compared to benign lesions) originating from the deep stromal conjunctiva. The lymphoma case shows remarkably dilated and deep episcleral vessel involvement, not seen in the BRLH lesions, and AS-OCTA could be potentially useful when assessing these lesions, which are clinically difficult to distinguish. However, a larger number of subjects in each category are necessary to confirm if the peri-lesional vascular changes described herein represent an early malignant sign of tumors and can be used as a complimentary diagnostic or monitoring tool.

Manual measurements of vessel depth and diameter can still carry some degree of subjectivity and is cumbersome for a clinical setting. Ideally, automated software for vessel analysis, such as diameter, depth, tortuosity and density, should be developed to further facilitate clinical implementation and ocular surface lesion assessment. Additionally, development of OCTA software specific for anterior segment is necessary to minimize artifacts and optimize image segmentation for analysis. It has been shown that different scan frame sizes and thresholding methods can significantly affect the quantitative analysis and should be considered in future AS-OCTA studies [34,35]. Nevertheless, in this study we also provided morphological vascular description that may further facilitate lesion assessment, without the time-consuming manual measurements. Of note, we have not evaluated other tumor properties in this study and is important to address in future studies.

The main limitations of this study are its retrospective nature and small sample size in each group, not allowing detailed analysis within each tumor subcategory. Nevertheless, our main goal was to further explore the utility of AS-OCTA in a variety of conjunctival lesions commonly presented at the clinic. Another limitation is the penetration of the spectral domain wavelength in dense tissues. It has been reported on AS-OCT that pigmented tumors may cause shadowing and possibly limit the visualization of the intra-lesional features, specifically in densely pigmented lesions [9,11,36]. In light of this, the peri-lesional vascular parameters presented herein may be further useful, since these are always visible through the semi-transparent conjunctiva. Of note, although ROC curves showed high AUC of the vascular parameters, the small number of patients in this study warrants further studies to confirm these findings. Lastly, imaging thick and extensive lesions can be challenging due to the limitations of commercially available devices. Thus, further technological advances should improve scan size, segmentation and image artifacts in order to provide more objective and automated vascular parameters for anterior segment of the eye.

In conclusion, this study demonstrated the AS-OCTA is capable of imaging and measuring the vessels in a variety of conjunctival lesions with high repeatability. Moreover, based on the evaluation of 3 prominent vessels for each lesion, malignant lesions showed significantly greater peri-lesional vessel depth and diameter compared to benign lesions and might be important diagnostic marker in ocular surface lesions, specifically in epithelial and pigmented lesions. Therefore, AS-OCTA provides a promising quantitative and non-invasive

tool to help assess ocular surface lesions and future studies are necessary to confirm our findings and to further explore its implementation for the clinician.

Supplementary Material

Refer to Web version on PubMed Central for supplementary material.

Acknowledgements

The authors would like to acknowledge Drs Michael Raizman, Michael Goldstein and Kenneth Kenyon for their contributions with their patients' clinical charts.

Funding

Massachusetts Lions Eye Research Fund, Inc. (PH), Research to Prevent Blindness Challenge Grant to the Department of Ophthalmology, Tufts Medical Center Institutional Support (PH). The funding organizations had no role in the design or conduct of this research.

References

[1]. Shields CL, Shields JA. Tumors of the conjunctiva and cornea. Surv Ophthalmol 2004;49(1):3–24. [PubMed: 14711437]

[2]. Shields CL, Demirci H, Karatza E, Shields JA. Clinical survey of 1643 melanocytic and nonmelanocytic conjunctival tumors. Ophthalmology 2004;111(9):1747–54. [PubMed: 15350332]

[3]. Shields JA, Shields CL, Gunduz K, Eagle RC Jr. The 1998 Pan American Lecture. Intraocular invasion of conjunctival squamous cell carcinoma in five patients. Ophthalmic Plast Reconstr Surg 1999;15(3):153–60. [PubMed: 10355832]

[4]. Gichuhi S, Macharia E, Kabiru J, et al. Clinical presentation of ocular surface squamous neoplasia in Kenya. JAMA Ophthalmol 2015;133(11):1305–13. [PubMed: 26378395]

[5]. Mahoney MC, Burnett WS, Majerovics A, Tanenbaum H. The epidemiology of ophthalmic malignancies in New York State. Ophthalmology 1990;97(9):1143–7. [PubMed: 2234844]

[6]. Shields CL, Alset AE, Boal NS, et al. Conjunctival tumors in 5002 cases. Comparative analysis of benign versus malignant counterparts. The 2016 james D. Allen lecture. Am J Ophthalmol 2017;173:106–33. [PubMed: 27725148]

[7]. Char DH, Kundert G, Bove R, Crawford JB. 20 MHz high frequency ultrasound assessment of scleral and intraocular conjunctival squamous cell carcinoma. Br J Ophthalmol 2002;86(6):632–5. [PubMed: 12034684]

[8]. Conway RM, Chew T, Golchet P, Desai K, Lin S, O'Brien J. Ultrasound biomicroscopy: role in diagnosis and management in 130 consecutive patients evaluated for anterior segment tumours. Br J Ophthalmol 2005;89(8):950–5. [PubMed: 16024841]

[9]. Bianciotto C, Shields CL, Guzman JM, et al. Assessment of anterior segment tumors with ultrasound biomicroscopy versus anterior segment optical coherence tomography in 200 cases. Ophthalmology 2011;118(7):1297–302. [PubMed: 21377736]

[10]. Krema H, Santiago RA, Gonzalez JE, Pavlin CJ. Spectral-domain optical coherence tomography versus ultrasound biomicroscopy for imaging of nonpigmented iris tumors. Am J Ophthalmol 2013;156(4):806–12. [PubMed: 23876869]

[11]. Janssens K, Mertens M, Lauwers N, de Keizer RJ, Mathysen DG, De Groot V. To study and determine the role of anterior segment optical coherence tomography and ultrasound biomicroscopy in corneal and conjunctival tumors. J Ophthalmol 2016;2016:1048760. [PubMed: 28050274]

[12]. Mueller AJ, Freeman WR, Folberg R, et al. Evaluation of microvascularization pattern visibility in human choroidal melanomas: comparison of confocal fluorescein with indocyanine green angiography. Graefes Arch Clin Exp Ophthalmol 1999;237(6):448–56. [PubMed: 10379603]

[13]. Stanga PE, Lim JI, Hamilton P. Indocyanine green angiography in chorioretinal diseases: indications and interpretation: an evidence-based update. Ophthalmology 2003;110(1):15–21. [PubMed: 12511340]

[14]. Brunner M, Steger B, Romano V, et al. Identification of feeder vessels in ocular surface neoplasia using indocyanine green angiography. Curr Eye Res 2018;43(2):163–9. [PubMed: 29111820]

[15]. Izatt JA, Hee MR, Swanson EA, et al. Micrometer-scale resolution imaging of the anterior eye in vivo with optical coherence tomography. Arch Ophthalmol 1994;112(12):1584–9. [PubMed: 7993214]

[16]. Nanji AA, Sayyad FE, Galor A, Dubovy S, Karp CL. High-resolution optical coherence tomography as an adjunctive tool in the diagnosis of corneal and conjunctival pathology. Ocul Surf 2015;13(3):226–35. [PubMed: 26045235]

[17]. Sambhav K, Grover S, Chalam KV. The application of optical coherence tomography angiography in retinal diseases. Surv Ophthalmol 2017;62(6):838–66. [PubMed: 28579550]

[18]. Lang SJ, Cakir B, Evers C, Ludwig F, Lange CA, Agostini HT. Value of optical coherence tomography angiography imaging in diagnosis and treatment of hemangioblastomas in von Hippel-lindau disease. Ophthalmic Surg Lasers Imaging Retina 2016;47(10):935–46. [PubMed: 27759860]

[19]. Sagar P, Rajesh R, Shanmugam M, Konana VK, Mishra D. Comparison of optical coherence tomography angiography and fundus fluorescein angiography features of retinal capillary hemangioblastoma. Indian J Ophthalmol 2018;66(6):872–6. [PubMed: 29786009]

[20]. Ang M, Sim DA, Keane PA, et al. Optical coherence tomography angiography for anterior segment vasculature imaging. Ophthalmology 2015;122(9):1740–7. [PubMed: 26088621]

[21]. Ang M, Cai Y, MacPhee B, et al. Optical coherence tomography angiography and indocyanine green angiography for corneal vascularisation. Br J Ophthalmol 2016;100(11):1557–63. [PubMed: 26823396]

[22]. Zhang M, Hwang TS, Campbell JP, et al. Projection-resolved optical coherence tomographic angiography. Biomed Opt Express 2016;7(3):816–28. [PubMed: 27231591]

[23]. Schindelin J, Arganda-Carreras I, Frise E, et al. Fiji: an open-source platform for biological-image analysis. Nat Methods 2012;9(7):676–82. [PubMed: 22743772]

[24]. Meyer PA, Watson PG. Low dose fluorescein angiography of the conjunctiva and episclera. Br J Ophthalmol 1987;71(1):2–10. [PubMed: 3814565]

[25]. Dawson Dgu JL, Edelhauser HF, SF. E.. Cornea and sclera. In: Levin LAN, Ver Hoeve J, Wu SM, editors. Adler's physiology of the eye. eleventh ed. Elsevier, Inc.; 2011. p. 71–163.

[26]. Zhang X, Li Q, Liu B, et al. In vivo cross-sectional observation and thickness measurement of bulbar conjunctiva using optical coherence tomography. Invest Ophthalmol Vis Sci 2011;52(10):7787–91. [PubMed: 21873655]

[27]. Read SA, Alonso-Caneiro D, Vincent SJ, et al. Anterior eye tissue morphology: scleral and conjunctival thickness in children and young adults. Sci Rep 2016;6:33796. [PubMed: 27646956]

[28]. McDonald DM, Choyke PL. Imaging of angiogenesis: from microscope to clinic. Nat Med 2003;9(6):713–25. [PubMed: 12778170]

[29]. Kwiterovich KA, Maguire MG, Murphy RP, et al. Frequency of adverse systemic reactions after fluorescein angiography. Results of a prospective study. Ophthalmology 1991;98(7):1139–42. [PubMed: 1891225]

[30]. Obana A, Miki T, Hayashi K, et al. Survey of complications of indocyanine green angiography in Japan. Am J Ophthalmol 1994;118(6):749–53. [PubMed: 7977601]

[31]. Liu Z, Karp CL, Galor A, Ai Bayyat GJ, Jiang H, Wang J. Role of optical coherence tomography angiography in the characterization of vascular network patterns of ocular surface squamous neoplasia. Ocul Surf 2020;S1542–0124(20):30062–8.

[32]. Ferrara N VEGF and the quest for tumour angiogenesis factors. Nat Rev Canc 2002;2(10):795–803.

[33]. Hongu T, Funakoshi Y, Fukuhara S, et al. Arf6 regulates tumour angiogenesis and growth through HGF-induced endothelial beta1 integrin recycling. Nat Commun 2015;6:7925. [PubMed: 26239146]

[34]. Binotti WW, Romano AC. Projection-resolved optical coherence tomography angiography parameters to determine severity in diabetic retinopathy. Invest Ophthalmol Vis Sci 2019;60(5):1321–7. [PubMed: 30933259]

[35]. Mehta N, Liu K, Alibhai AY, et al. Impact of binarization thresholding and brightness/contrast adjustment methodology on optical coherence tomography angiography image quantification. Am J Ophthalmol 2019;205:54–65. [PubMed: 30885708]

[36]. Shields CL, Belinsky I, Romanelli-Gobbi M, et al. Anterior segment optical coherence tomography of conjunctival nevus. Ophthalmology 2011;118(5):915–9. [PubMed: 21146221]

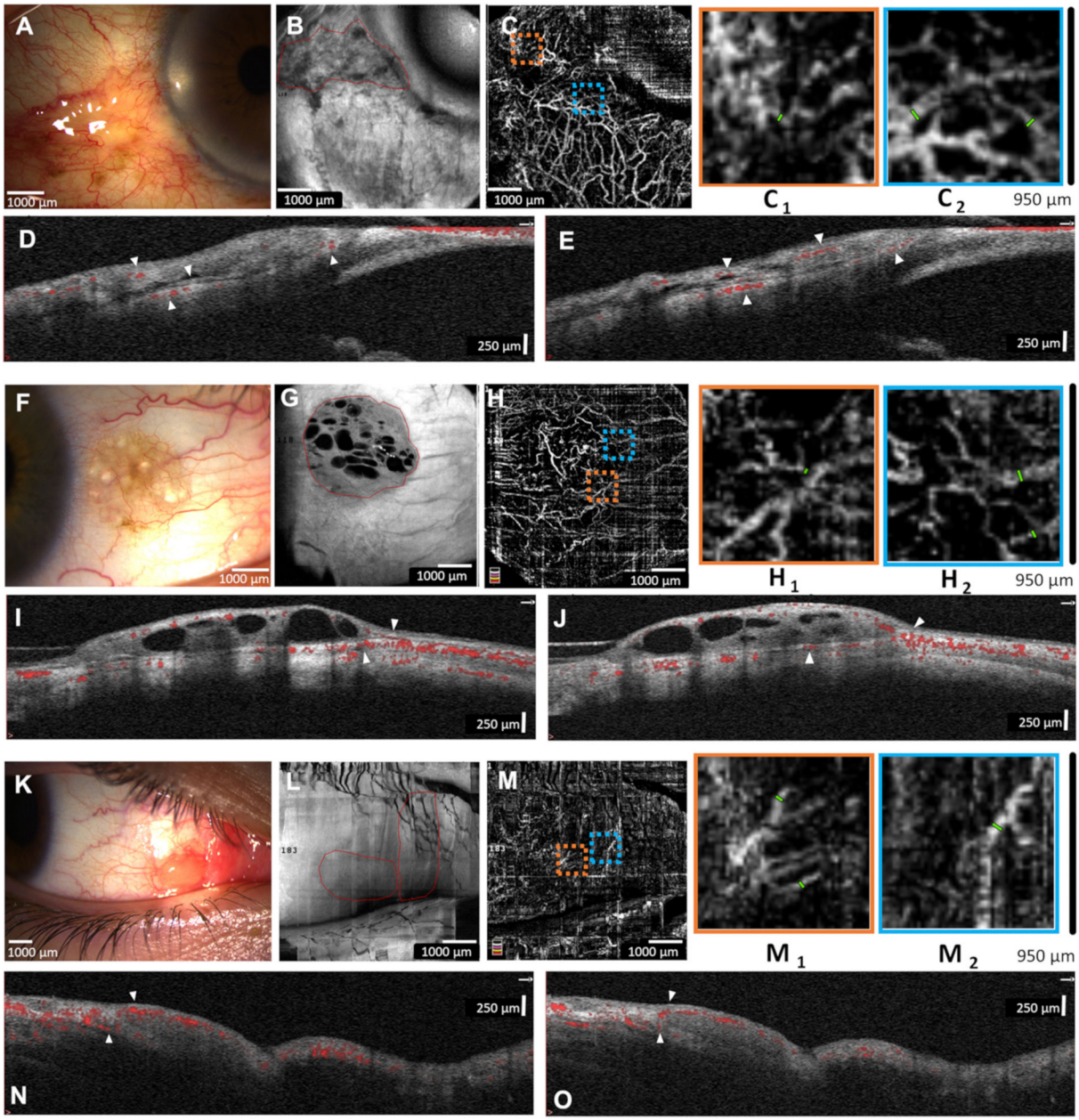

Fig. 1.

Representative images from benign lesions. A) Slit-lamp photograph of a 78-year-old male with an inflamed pinguecula of the left eye. B) *En face* AS-OCT showing lesion borders. C) AS-OCTA shows the conjunctival and scleral vasculature with magnified areas (950 × 950 µm orange and blue boxes; C_1 and C_2, respectively) to highlight peri-lesional vessel measurement. D and E) AS-OCT B-lines shows superficial and deep stroma conjunctival vessels that respect the conjunctival inferior border (arrowheads). F) Slit-lamp photograph of a 39-year-old male with a cystic conjunctival nevus of the right eye. G) *En face* AS-OCT shows lesion borders and intra-lesional cysts. H) AS-OCTA shows normal conjunctival vessels surrounding the lesion (H_1 and H_2). I and J) AS-OCT B-lines highlight superficial conjunctival vessels entering lesion with normal underlying deep conjunctival and episcleral

vessels (arrowheads). K) Slit-lamp photograph of a 15-year-old male with benign reactive lymphoid hyperplasia (BRLH) of the right eye. L*) En face* AS-OCT show lesion borders. M) AS-OCTA shows thin conjunctival vessels surrounding lesion (M_1 and M_2). N and O) AS-OCT B-lines show superficial conjunctival vessels overlying lesions and few underlying deep conjunctival vessels without branching (arrowheads).

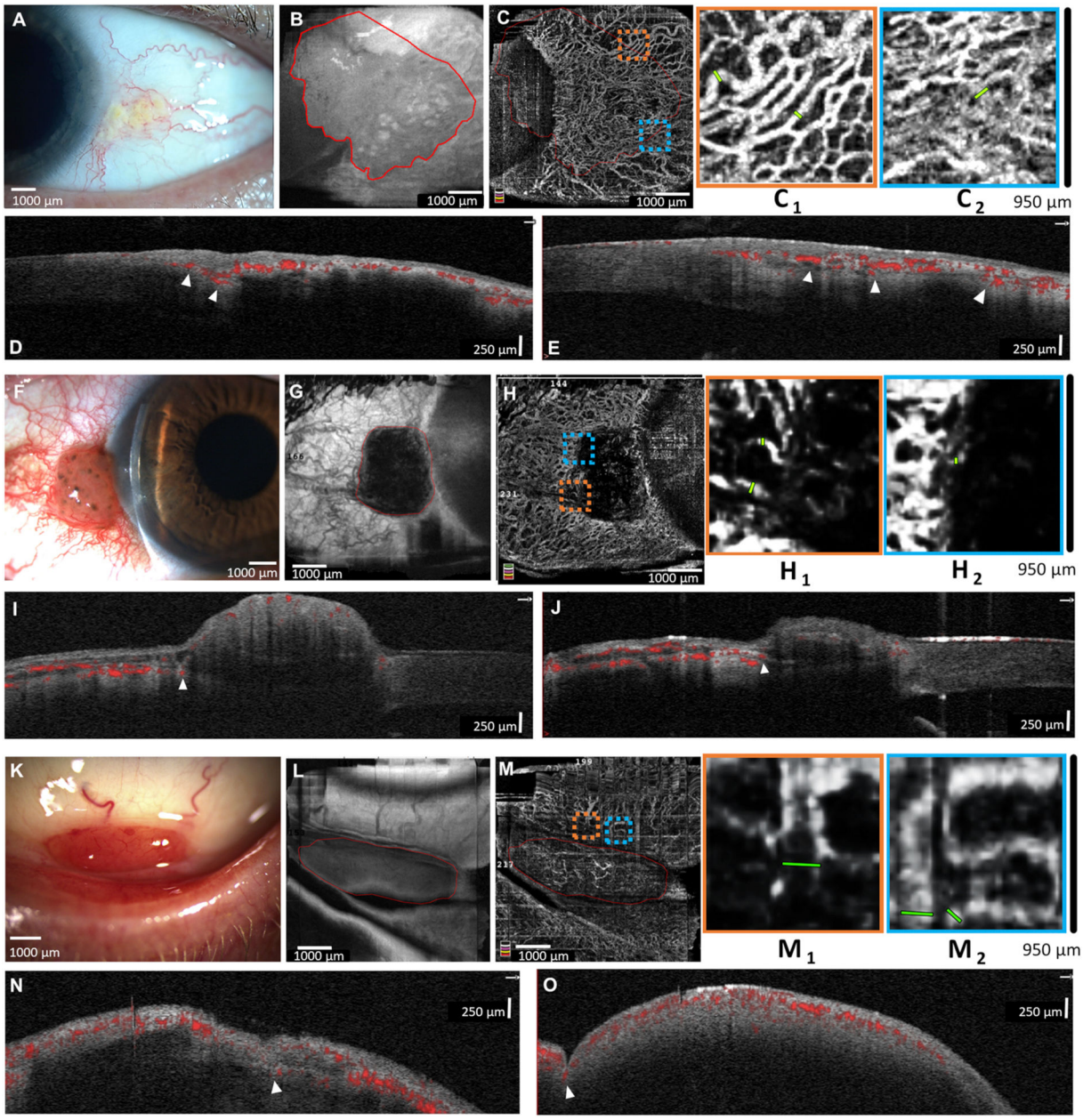

Fig. 2.

Representative images from malignant lesions. A) Slit-lamp photograph of a 58-year-old male with a conjunctival intra-epithelial neoplasia (CIN) of left eye. B) *En face* AS-OCT shows the lesion borders. C) AS-OCTA shows a highly vascularized conjunctiva, highlighting dilated peri-lesional vessels (C_1 and C_2). D and E) AS-OCT B-lines show the intra-lesional vessels are highly connected to the deep conjunctival and episcleral vessels at the lesion base (arrowheads). F) Slit-lamp photograph of a 59-year-old male with conjunctival melanoma of the right eye. G) *En face* AS-OCT shows lesion borders. H) AS-OCTA shows many peri-lesional vessels (highlighted in H_1 and H_2) with scant intra-lesional vessels. I and J) AS-OCT B-lines show superficial conjunctival vessels overlying lesion with deep episcleral branches entering lesion base (arrowheads). K) Slit-lamp photograph

of a 64-year-old male with bilateral lymphoma in the inferior fornix. L) *En face* AS-OCT shows the lesion borders. M) AS-OCTA shows many peri-lesional vessels (highlighted in M_1 and M_2) and fine vessels overlying the lesion. N and O) AS-OCT B-lines highlight deep episcleral vessels entering the lesion base (arrowheads). All malignant lesions were biopsy proven.

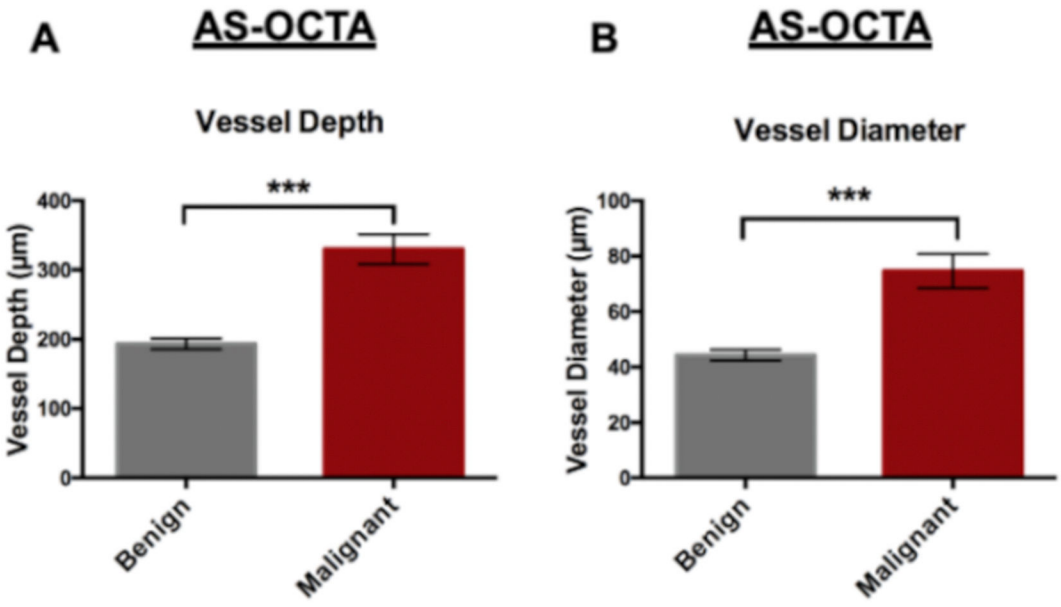

Fig. 3.

Bar graphs of the AS-OCTA parameters between benign and malignant conjunctival lesions show vessel depth (A) and vessel diameter (B). Generalized estimated equations with Bonferroni correction ($p \leq 0.001$***).

Table 1

Demographics of benign and malignant lesions.

Lesion Classification	Ocular Surface Lesion	
	Benign	Malignant
Epithelial (N)	8 (35%)	5 (50%)
Pterygium/Pingueculae	8 (61%)	
CIN		4 (31%)
Invasive OSSN		1 (8%)
Pigmented (N)	7 (30%)	3 (30%)
Nevus	6 (60%)	
Complex-Associated Melanosis	1 (10%)	
PAM with Atypia/Melanoma *in situ*		1 (10%)
Melanoma		2 (20%)
Lymphoid (N)	8 (35%)	2 (20%)
BRLH	4 (40%)	
Conjunctival Granuloma	2 (20%)	
Conjunctival Inclusion Cysts	2 (20%)	
Lymphoma		2 (20%)
Total Eyes N	23 (100%)	10 (100%)

Conjunctival intra-epithelial neoplasia (CIN), ocular surface squamous neoplasia (OSSN), primary acquired melanosis (PAM) and benign reactive lymphoid hyperplasia (BRLH).

Table 2

Parameters between benign and malignant ocular surface lesions as sub-categorized by lesion type.

Parameters	Benign Lesions	Malignant Lesions	P Value
Epithelial lesions (subjects)	8 (8)	5 (5)	
Vessel Depth (μm)	192.5 ± 25.4	271.7 ± 56.7	0.005
Vessel Diameter (μm)	44.8 ± 7.3	73.5 ± 15.3	0.003
Pigmented lesions (subjects)	7 (7)	3 (3)	
Vessel Depth (μm)	177.0 ± 49.6	308.9 ± 49.0	0.036
Vessel Diameter (μm)	38.9 ± 6.2	70.1 ± 14.2	0.036
Lymphoid lesions (subjects)	8 (7)	2 (1)	
Vessel Depth (μm)	221.4 ± 8.6	429.2 ± 5.3	-
Vessel Diameter (μm)	46.9 ± 12.2	102.9 ± 7.2	-